

# Osteoarthritis and Cartilage



## Bone marrow lesions identified by MRI in knee osteoarthritis are associated with locally increased bone mineral density measured by QCT



T. Lowitz<sup>†,\*</sup>, O. Museyko<sup>†</sup>, V. Bousson<sup>‡,§</sup>, L. Laouisset<sup>‡,§</sup>, W.A. Kalender<sup>†</sup>, J.-D. Laredo<sup>‡,§</sup>, K. Engelke<sup>†</sup>

<sup>†</sup> Institute of Medical Physics, University of Erlangen-Nuernberg, Henkestr. 91, 91052 Erlangen, Germany

<sup>‡</sup> Service de Radiologie OstéoArticulaire, Assistance Publique-Hôpitaux de Paris, Hôpital Lariboisière 2 rue Ambroise Paré, 75010 Paris, France

<sup>§</sup> Université Paris Diderot, Paris, France

### ARTICLE INFO

#### Article history:

Received 20 September 2012

Accepted 9 April 2013

#### Keywords:

Bone marrow lesions  
Quantitative computed tomography  
Bone mineral density  
Magnetic resonance imaging  
Segmentation  
Registration

### SUMMARY

**Objective:** Bone marrow lesions (BMLs) in the knee are associated with pain and compartment-specific joint space narrowing. However, the correlation of BMLs with bone mineral density (BMD) has rarely been investigated. The aim of the present study was to examine whether BMD in BMLs is altered compared to the surrounding bone.

**Design:** Thirty-four BMLs detected in osteoarthritis (OA) knees (KL grade 2 and 3) of 26 patients were investigated. A 3D-segmentation was used to determine BML volumes of interest (VOI) and their surrounding bone in MR images. These VOIs were registered to corresponding single-energy QCT images and a BMD analysis was performed. The same VOIs were transferred to control datasets (19 OA patients without BMLs) by an elastic registration, where the BMD analysis was repeated. To account for the dependence of bone marrow composition on BMD measures derived using single-energy QCT, simulations were performed to evaluate how changing fat-water compositions likely occurring with BML development may influence BMD measures and observed BMD differences between patients with and without BMLs. The association between loading in the knee and the occurrence of BMLs was investigated by medial to lateral (M:L) BMD ratios.

**Results:** BMD was significantly increased at BML locations, even with a fat-to-water conversion rate of 39%. The M:L BMD ratio was significantly increased in bones with medial BMLs.

**Conclusions:** BMD was examined exactly at BML locations and surrounding bone using highly accurate segmentation and registration methods. BMD was significantly increased at BML locations ( $P < 0.05$ ).

© 2013 Osteoarthritis Research Society International. Published by Elsevier Ltd. All rights reserved.

### Introduction

Cartilage deterioration is a major focus in osteoarthritis (OA) and attracts most of the research attention in knee OA. However, cartilage is not a source of pain, as it does not contain nociceptors. In contrast, bone marrow lesions (BMLs) in the knee are strongly associated with pain<sup>1,2</sup>, but also with compartment-specific cartilage degeneration<sup>3,4</sup>. Therefore, BMLs are a very interesting target

in diagnosis and monitoring of OA<sup>5–7</sup>. In addition, they can be relatively easily detected as high signal intensity regions on T2-weighted fat-suppressed images. During OA progression, the subchondral bone architecture changes, which affects its ability to absorb and dissipate energy causing BMD<sup>8,9</sup> and cartilage changes<sup>10,11</sup>. Interestingly, the association of BMLs with local BMD has rarely been investigated<sup>12–14</sup> and as of today there is no consensus whether a BMD increase or decrease is expected in BMLs. Two opposing hypotheses exist. In a study using histology, Zanetti *et al.*<sup>15</sup> showed that BMLs included several bone tissue abnormalities such as bone marrow necrosis and fibrosis (confirmed by Kazakia *et al.*<sup>14</sup> and Modic and Ross<sup>16</sup>), as well as necrotic and remodeled trabeculae. These tissue composition changes suggest ongoing response to a local injury in the form of trabecular microcracks suggesting that BMLs may originate in regions with low bone strength marked by low numbers of trabeculae or low

\* Address correspondence and reprint requests to: T. Lowitz, Institute of Medical Physics, University of Erlangen-Nuernberg, Henkestr. 91, 91052 Erlangen, Germany. Tel: 49-9131-8525530.

E-mail addresses: Torsten.Lowitz@imp.uni-erlangen.de (T. Lowitz), Oleg.Museyko@imp.uni-erlangen.de (O. Museyko), valerie.bousson@lrp.aphp.fr (V. Bousson), lieusslaouisset@hotmail.com (L. Laouisset), Willi.Kalender@imp.uni-erlangen.de (W.A. Kalender), jean-denis.laredo@lrp.aphp.fr (J.-D. Laredo), Klaus.Engelke@imp.uni-erlangen.de (K. Engelke).

mineral content (both indicative of low BMD). A second hypothesis is that BMLs occur preferably in subchondral trabecular bone regions under increased loading<sup>3</sup>, which also induces increased BMD in the same areas<sup>17,18</sup>.

To our best knowledge, only three previous studies investigated the relationship between BMLs and local BMD. Lo *et al.*<sup>12</sup> studied the relationship between the medial to lateral (M:L) tibial plateau BMD ratio and the BML occurrence. Medial tibial plateau BMLs were associated with increased M:L BMD ratio. The authors concluded that local BMD was increased in BMLs. A limitation of this study was the use of DXA to determine BMD and especially the size of the regions of interest (ROIs) which widely exceeded that of the BMLs. In addition, the ROIs included both cortical and cancellous bone while BMLs affect cancellous bone only. Finally, the influence of the fat-to-water ratio of the bone marrow on BMD results was not addressed in this study. This is especially critical if the fat-to-water ratio changes, such as in BMLs where bone marrow fat is partly replaced by water<sup>19,20</sup>. These inaccuracies due to bone marrow content changes affect both DXA and single-energy QCT<sup>21,22</sup>.

Hunter *et al.*<sup>13</sup> examined bone samples from medial tibial plateaus with BMLs obtained from total knee replacements in six postmenopausal women. They used micro-CT to compare tissue mineral density (TMD) and bone volume as a percentage of tissue volume (BV/TV) in cylindrical cores extracted from four different volumes of interest (VOIs) in the subchondral bone, namely BML VOIs, lesion-free VOIs from the same (medial) tibial plateau, as well as matched VOIs in the lateral plateau. BV/TV in the lesions was significantly higher than in the matched lesion-free VOI from the lateral tibial plateau, but TMD was not. BV/TV and TMD in the lesions were also higher than in the neighboring bone of the medial tibial plateau. Limitations of the study were the small sample size, the fact that intra-compartmental M:L BV/TV and TMD ratios were not considered and that multiple samples were taken from the same BML.

Kazakia *et al.*<sup>14</sup> performed micro-CT and high-resolution peripheral QCT (HR-pQCT) investigations of the tibial plateau in 10 specimens from six donors, which were collected during total knee arthroplasty. Like Hunter, they reported an increase in BV/TV in BMLs. They did not detect a significant difference in TMD between BML and non-BML tissue, but a significant increase in volumetric BMD measured in micro-CT as well as in HR-pQCT datasets.

The aim of the *in vivo* study presented here was to examine whether BMD measured exactly at the BML location was altered when compared to the surrounding cancellous bone.

## Methods

### Patients

Forty-five patients with primary knee OA (KL grade 2 or 3) were included in the study. The BML group consisted of 26 patients (24 females:  $62 \pm 8$  years, two males:  $70 \pm 8$  years) with 34 BMLs (WORMS grade  $\geq 1$ , 19 in the femur and 15 in the tibia). The control group consisted of 19 knee OA patients (14 females:  $63 \pm 8$  years, five males:  $66 \pm 13$  years) without BMLs. All patients participated in the CT substudy of the longitudinal multicenter Polka study, which investigated the effect of strontium ranelate on knee OA<sup>23</sup>. The ethics approval for the CT substudy was received from the *Comité de protection des personnes* (CPP) d'Ile de France (Hôpital Saint Antoine, Paris APHP, France). In the current investigation, only baseline data from three different centers were used. Therefore, none of the 45 patients had received strontium ranelate prior to image acquisition. All patients had suffered from knee pain during most days in the month before the CT investigation (intensity  $\geq 40$  mm on a visual analog scale) and had joint space widths between 2.5 mm and 5 mm. The BMLs were detected by a consensus reading of two

expert musculoskeletal radiologists (VB and JDL). The patients of the control group were randomly selected from all patients participating in the substudy who had no BML.

### Image acquisition

MR as well as CT data were acquired from the same knee. All MR datasets were acquired on Siemens MAGNETOM Avanto scanners with the following protocol: 1.5 T, extremity coil, T2-weighted fat-saturated coronal turbo spin echo sequence, TR/TE: 3,000 ms–5,290 ms/31 ms–41 ms, slice thickness 3 mm,  $256 \times 256$  matrix, field of view 14 cm. CT data were acquired on a Siemens Sensation 4, a Siemens Volume Zoom or a Siemens Sensation 64 all using the following protocol: 120 kV, 250 mAs, slice thickness 0.5 mm, reconstruction increment 0.3 mm, field of view 13 cm, scan range 20 cm, effective dose below 0.15 mSv. Additionally, an in-scan calibration phantom (Siemens OSTEO phantom) was placed beneath the target knee during the image acquisition in order to convert CT values to BMD. Voxel dimensions in coronal, sagittal and transversal directions of the MR data were  $0.55 \times 3.00 \times 0.55$  mm<sup>3</sup>, respectively, and  $0.25 \times 0.25 \times 0.30$  mm<sup>3</sup> for the CT data. Central quality control of all CT and MR exams was performed by the same radiologist from one of the participating centers.

### Image analysis (segmentation)

The analysis procedure started with an automatic 3D-segmentation of the distal femur and proximal tibia in the CT datasets [Fig. 1(b)] using 3D volume growing with local adaptive thresholds and morphological operations<sup>24</sup>. The next step was a multi-modality rigid registration of the segmented bone VOIs from the CT to the corresponding MR datasets [Fig. 1(a)]. The accuracy of this registration process was examined by calculating the Mattes mutual information (MMI)<sup>25</sup>. MMI absolute values depend on the exact registration settings and therefore cannot directly be used to determine the registration quality. In order to grade the CT-MR registration quality after registration, the MR dataset was artificially translated and rotated out of its optimal position (Fig. 5). The MMI value for the CT-MR rigid registrations was  $0.064 \pm 0.028$  (mean  $\pm$  standard deviation). Distorting the translation and rotation resulted in slightly lower MMI values of  $0.061 \pm 0.027$  and  $0.056 \pm 0.025$  for the two steps shown in Fig. 5. The Insight Segmentation and Registration Toolkit (ITK) library<sup>26</sup> was used for all registration processes.

The third step consisted of an automatic 3D-segmentation of the BMLs in the MR datasets, based on a user-defined seed point placed in each BML with subsequent volume growing. In case of unsatisfying results, the user could manually edit the segmentation<sup>27</sup>. Afterward, the resulting BML VOI was dilated and then the original BML VOI was subtracted from this dilated volume to obtain the neighborhood VOI. The final dilation advanced in successive minimal dilation steps until the volume ratio of neighborhood to BML VOI reached four. This number was selected empirically so that the volume of the resulting neighborhood VOI was large enough to include lesion-free trabecular bone tissue. At the same time for the majority of BMLs, the neighborhood VOI was sufficiently small not to include regions too far away from the BML. However, this was not the case for large BMLs [Fig. 2(a)]. Therefore, an alternative method consisting of a constant dilation distance of 2.75 mm in the x- and z-directions and of 3.00 mm in the y-direction was also used for all BMLs [Fig. 2(b)]. This second set of neighborhood VOIs was analyzed separately.

### Image analysis (BMD measurements)

For the BMD analysis, BML and neighborhood VOIs were registered back to the CT dataset. Dice ratios<sup>28</sup> which were calculated between

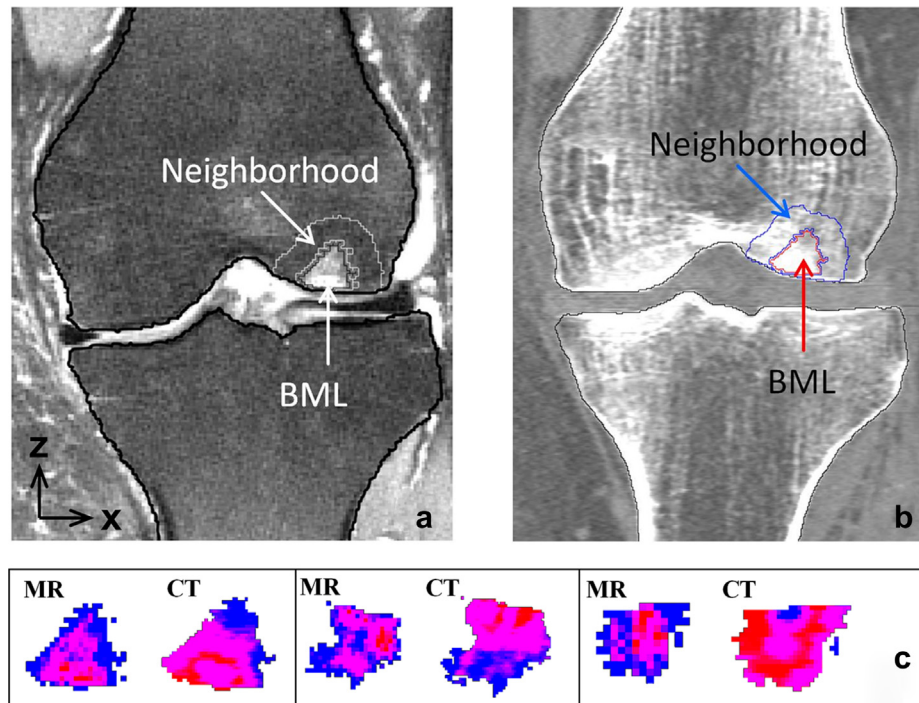


**Fig. 1.** (a) MR image with segmented BML and neighborhood VOI, (b) VOIs registered rigidly to CT image of the same knee, (c) color maps of MR signal intensity distribution vs BMD distribution in three BMLs (red corresponds to high signal intensity, blue to low signal intensity). The pair of color maps on the left corresponds to the BML shown in (a) and (b).

segmented and registered periosteal BVs in order to score the registration results were very high ( $0.962 \pm 0.017$ , mean  $\pm$  standard deviation). Mean BMD values were measured in the BML VOI ( $BMD_{BML}$ ) and in the neighborhood VOI ( $BMD_{neighborhood}$ ). As a figure of merit, the relative BMD difference  $\Delta BMD$  was calculated:

$$\Delta BMD = \frac{BMD_{BML} - BMD_{neighborhood}}{BMD_{neighborhood}} \quad (1)$$

Consistent with clinical knowledge, BMLs preferably occurred very close to the joint space. In order to compensate for BMD gradients in the proximal tibia and distal femur, the BMD analysis was repeated in corresponding regions of the control group.  $\Delta BMD$  in the BML and the control groups were combined as follows: first, an elastic CT–CT registration of the periosteal surface of a femur or tibia containing a BML to the corresponding bone of a randomly assigned control group dataset was performed (Fig. 3). Left knees

were registered on left knees and right knees on right knees. Second, the transformation matrix of the elastic CT–CT registration was used to register the BML and neighborhood VOIs to the control dataset. They were also labeled BML and neighborhood VOIs in the control datasets although no BML was present. As in the BML group,  $\Delta BMD$  values were calculated in the control group. For statistical purposes, each BML was registered on five different, randomly selected control group datasets. Then, for every BML, in each of the five corresponding control group datasets, BMD was calculated in the BML VOI and in the neighborhood VOI. Subsequently, BMD values from the five related control group datasets were averaged. Finally,  $\Delta BMD$  values were calculated for each BML using these averaged BMD values.

Since KL grades of BML knees were slightly higher compared to those of the control group used for the matching (2.5 vs 2.1), a KL-aligned sub-dataset was created in order to adjust for a potential effect of a difference in KL grades. This KL-aligned sub-dataset

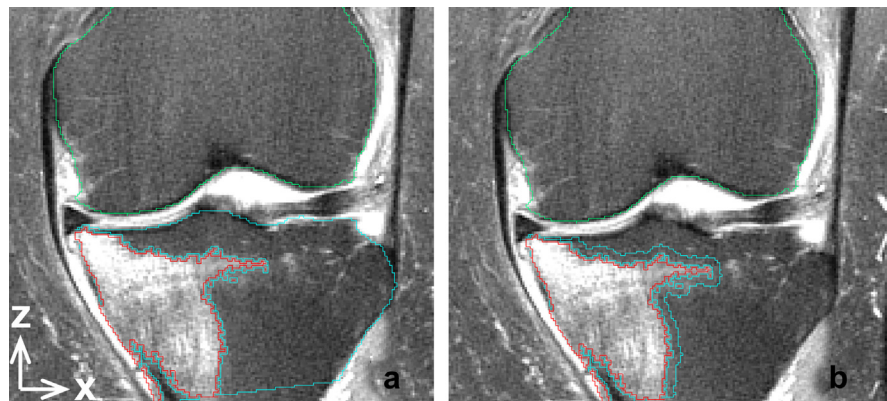


**Fig. 2.** (a) Neighborhood VOI four times the size of the BML VOI, (b) neighborhood VOI generated with a constant dilation from the BML VOI. Shown are the contour lines of the VOIs.



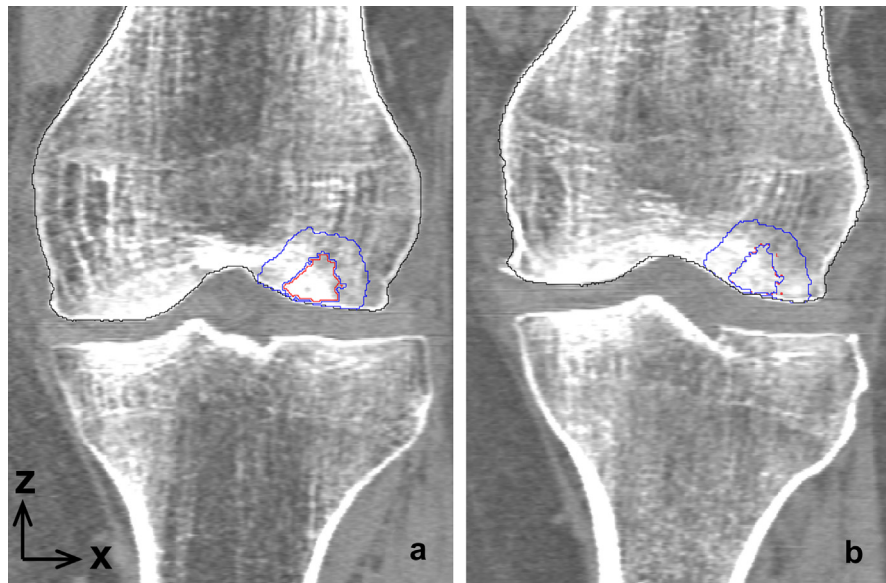


**Fig. 3.** (a) VOIs in CT image of BML group [compare Fig. 1(b)], (b) VOIs registered elastically to CT image of control knee (different shape) (BMD was calculated as the mean from five different randomly assigned control knees).

included only those BML-control dataset combinations in which the KL grade in the compartments containing a BML was equal or lower than in the corresponding compartments in the control knees.

#### Statistical analysis

One-sample *t*-tests were performed independently for the BML and the control group (34 BMLs each) to examine whether  $\Delta$ BMD was significantly different from zero. Afterward, a two-sample Student's *t*-test was performed to detect  $\Delta$ BMD differences between both groups. The use of the Student's *t*-test is based on the assumptions of independent observations, Gaussian distribution, and homogeneous variance. The latter two were tested by the Shapiro–Wilk and the Levene's tests, respectively. Several patients contributed more than one observation to the overall sample (six patients with two BMLs, one patient with three BMLs). This was a potential problem because multiple measurements on one patient are typically more similar than measurements on different patients<sup>29</sup>. Therefore, an additional statistical analysis was performed with averaging of within-patient measurements<sup>30</sup>. This resulted in even slightly higher  $\Delta$ BMD differences between the BML and the control group as between-patient variances were lower than within-patient variances. Therefore, as a conservative approach, we decided to treat the BMLs as independent observations during the statistical analysis. For all statistical tests a *P*-value of smaller than 0.05 was considered statistically significant. This statistical analysis was repeated with the KL-aligned sub-dataset.

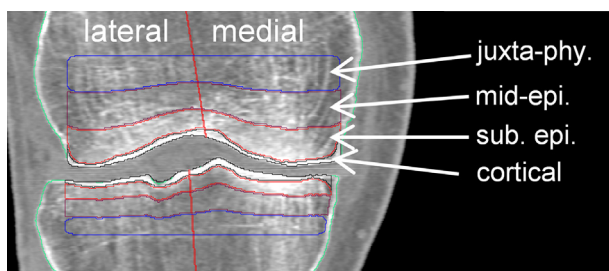


**Fig. 4.** CT image with analysis VOIs.

#### Fat-to-water conversion

As addressed earlier, single-energy QCT is affected by fat, which artificially lowers BMD<sup>21,22</sup>. In adults, the bone marrow of the femoral and tibial epiphyses almost exclusively consists of yellow marrow, i.e., fatty marrow<sup>31,32</sup>. Thus,  $\Delta$ BMD differences between the BML and the control groups may be artificially caused by a higher water and lower fat content in BML trabecular bone areas compared to BML-free areas. Therefore, the BMD effect of a change from fatty to water equivalent tissue within the BML was estimated using the following assumptions: CT-value of water 0 HU<sup>33</sup>, CT-value of fat –100 HU<sup>33</sup>, BV/TV = 0.15<sup>34</sup> and consequently a bone marrow content of 85%. Under the assumption that yellow marrow consists of about 80% fat<sup>32</sup>, this results in a fat content of 68% in BML-free trabecular bone areas. For the estimation, at first, the CT values were modified according to the desired fat-to-water conversion rate. Then, the new CT values were converted to BMD values by using the calibration equations. Thereby, the  $\Delta$ BMD difference between the BML and the control group was determined for decreasing fat-to-water ratios. Finally, the maximum fat-to-water ratio which still preserved significant  $\Delta$ BMD differences between BML and control groups was calculated.

#### Association between loading and BMLs

The association between loading in the knee joint (estimated using the M:L BMD ratio<sup>12</sup>) and the occurrence of BMLs was investigated. The M:L BMD ratio was calculated separately for the cortical, subchondral epiphyseal, mid-epiphyseal and juxta-physal VOIs<sup>24</sup> (Fig. 4), as well as in combinations of VOIs in order to investigate BMD ratios in larger VOIs. Further, the M:L BMD ratio was calculated separately for three groups: medial BMLs (*n* = 21), lateral BMLs (*n* = 13) and no BMLs (*n* = 34). The BMLs were classified as medial or lateral according to the VOIs they were located in. In knees with BMLs in the tibia (*n* = 15), only tibial VOIs were considered. In knees with BMLs in the femur (*n* = 19), only femoral VOIs were considered. The M:L BMD ratio in the matched knees without BMLs was calculated in the corresponding femoral (*n* = 19) and tibial VOIs (*n* = 15). An analysis of variance (ANOVA) was performed to detect differences between the three bone groups: medial BMLs, lateral BMLs and no BMLs. A post-hoc Tukey's HSD

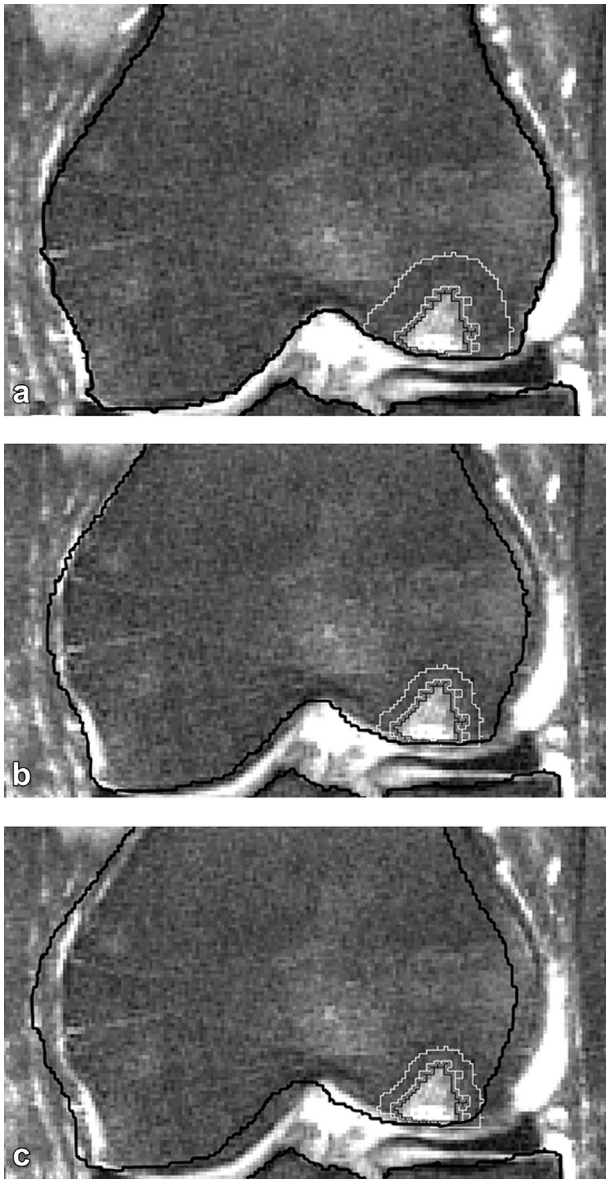


**Fig. 5.** CT-MR rigid registration. (a) Original, (b) and (c) manually translated and rotated to score MMI values.

(Honestly Significant Difference) test was performed to detect individual differences in M:L BMD ratios between the three groups and in order to adjust for multiple comparisons.

#### Analysis of BML characteristics

Lastly, we investigated relationships between (1) BML size and  $\Delta$ BMD; (2) heterogeneity (= standard deviation) of the BMD distribution in the BML VOI and BML size; and (3) heterogeneity of the BMD distribution in the BML VOI and KL grades. Linear regression analyses were performed for the first two relationships and a Student's *t*-test was performed to detect differences between the two groups (KL 2 and KL 3) of the latter relationship.

#### Results

The results of the CT-MR rigid registrations and the CT–CT elastic registrations of the periosteal surfaces are shown in Figs. 1 & 3, respectively.  $\Delta$ BMD was significantly different from zero in the

BML ( $P < 0.00001$ ) and in the control group ( $P < 0.001$ ). However,  $\Delta$ BMD was significantly higher in the BML ( $40.6\% \pm 37.4\%$ ; mean  $\pm$  standard deviation) compared to the control group ( $13.9\% \pm 21.1\%$ ). Larger changes in  $\Delta$ BMD were found when the neighborhood VOI was defined by a constant dilation distance. Here,  $\Delta$ BMD remained significantly different from zero in the BML group ( $22.7\% \pm 25.4\%$ ;  $P < 0.0001$ ) but no longer in the control group ( $2.3\% \pm 23.3\%$ ,  $P = 0.572$ ). The difference in  $\Delta$ BMD between both groups remained significant.

Results were not impacted by the additional condition that the KL grades in the control group datasets had to be higher or equal to the KL grades of the matched knee compartments with a BML. Under this condition,  $\Delta$ BMD in the BML group was  $39.5\% \pm 39.2\%$  compared to  $15.1\% \pm 21.6\%$  in the control group, i.e., hardly different from the  $\Delta$ BMD values obtained without this condition. Therefore, the random assignment process without consideration of specific compartmental KL grades was justified.

The results of the simulations of different fat-to-water ratios in the BMLs showed that the difference of  $\Delta$ BMD between BML and control group remained significant ( $P < 0.05$ ) under the assumption that no more than 39% of fat-equivalent material had been converted to water-equivalent material in the BML VOI. In this case,  $\Delta$ BMD in the BML group dropped from  $40.6\% \pm 37.4\%$  to  $28.1\% \pm 35.8\%$ . When the neighborhood VOI was defined by a constant dilation, the difference of  $\Delta$ BMD between BML and control group remained significant under the assumption that no more than 30% of fat-equivalent material had been converted to water-equivalent material in the BML VOIs.

Mean BMD values for all VOIs are presented in Table I. The M:L BMD ratios are shown in Table II. Corresponding *p*-values of the ANOVA and Tukey's HSD tests are presented in Table III. M:L BMD ratios were significantly higher in bones with medial BMLs compared to bones without BMLs (except for the cortical and juxta-physeal VOI) and compared to bones with lateral BMLs (except for the juxta-physeal VOI). Apart from the cortical VOI, differences between bones with lateral BMLs and bones without BMLs were not significant although the M:L BMD ratio was numerically lower in the bones with lateral BMLs.

No significant linear relationships or group differences were noted between (1) BML size and  $\Delta$ BMD ( $P = 0.07$ ); (2) BMD heterogeneity and BML size ( $P = 0.50$ ); and (3) BMD heterogeneity and KL grades ( $P = 0.76$ ).

#### Discussion

The main finding of the present study was an increased BMD in BML VOIs compared to the surrounding trabecular bone. The increase in  $\Delta$ BMD was significantly higher in the BML group compared to the BML-free control group. In locations where BMLs were found, BMD was also increased in the control group with knee OA but without lesions. The increased BMD in the control group was caused by the preferred occurrence of BMLs in proximity of the joint space. The difference of  $\Delta$ BMD between BML and control groups remained significant even when the dilation with a constant distance was used, which resulted in a significant decrease of the neighborhood VOI volume, in particular for large BMLs (Fig. 2). In this case, the surrounding bone was limited to a region very close to the BML where BMD could still be influenced by the BML. However, with this approach the BMD gradients had less impact on  $\Delta$ BMD. Not surprisingly,  $\Delta$ BMD depended on the neighborhood VOI volume.

The high signal intensity of BML areas on T2-weighted MR sequences suggests increased local water content. A change in bone marrow composition compared to lesion-free trabecular bone tissue artificially increased BMD values as measured by QCT<sup>21,22</sup> and

**Table I**  
BMD values as mean  $\pm$  standard deviation for S1 (subchondral epiphyseal), S2 (mid-epiphyseal), S3 (juxta-physeal) and cortical VOIs in the femur or tibia (according to BML location), respectively (compare Fig. 4)

VOI	Medial BMLs		No BMLs		Lateral BMLs	
	Medial	Lateral	Medial	Lateral	Medial	Lateral
Cortical	523 $\pm$ 67	423 $\pm$ 69	516 $\pm$ 69	447 $\pm$ 68	511 $\pm$ 85	503 $\pm$ 67
S1	288 $\pm$ 53	215 $\pm$ 69	295 $\pm$ 50	261 $\pm$ 55	277 $\pm$ 56	269 $\pm$ 46
S2	161 $\pm$ 42	135 $\pm$ 61	182 $\pm$ 36	176 $\pm$ 53	164 $\pm$ 35	174 $\pm$ 41
S3	123 $\pm$ 37	105 $\pm$ 57	140 $\pm$ 31	140 $\pm$ 51	132 $\pm$ 30	139 $\pm$ 42
Cortical + S1	357 $\pm$ 63	284 $\pm$ 69	364 $\pm$ 54	323 $\pm$ 52	337 $\pm$ 70	340 $\pm$ 63
Cortical + S1 + S2	260 $\pm$ 49	211 $\pm$ 61	274 $\pm$ 41	250 $\pm$ 49	251 $\pm$ 50	257 $\pm$ 46
Cortical + S1 + S2 + S3	216 $\pm$ 43	177 $\pm$ 59	232 $\pm$ 36	216 $\pm$ 47	212 $\pm$ 44	218 $\pm$ 42
S1 + S2	210 $\pm$ 44	166 $\pm$ 64	227 $\pm$ 38	210 $\pm$ 53	208 $\pm$ 42	208 $\pm$ 42
S1 + S2 + S3	179 $\pm$ 40	144 $\pm$ 61	196 $\pm$ 34	185 $\pm$ 50	180 $\pm$ 37	182 $\pm$ 42
S2 + S3	141 $\pm$ 38	121 $\pm$ 59	162 $\pm$ 32	159 $\pm$ 50	146 $\pm$ 33	155 $\pm$ 42

the question remained whether the observed increase in  $\Delta$ BMD and in particular the difference of  $\Delta$ BMD between BML and control groups could be explained by a change in the fat-water ratio. Simulations were carried out to estimate the effect of a change in bone marrow content on  $\Delta$ BMD. For this purpose, the absorption characteristics of a varying number of voxels within the BML were changed from fat to water.  $\Delta$ BMD was significantly higher in the BML group compared to the control group as long as no more than 39% (30% for alternative definition of neighborhood VOI) of the voxels within the BML were converted from fat to water. Although the histology of BMLs has not been quantified yet, except by Zanetti *et al.*<sup>15</sup>, a fat-to-water conversion rate of even 30% seems rather high. It is not known in which proportion fatty tissue is replaced by hydrated tissue in BML areas. However, it is well known that BMLs are usually labile and return to a normal fatty signal intensity after some months or sometimes years, which suggests that part of the fat is retained in the bone marrow of the BML areas.

In agreement with the previous report by Lo *et al.*<sup>12</sup>, we found an association between the occurrence of BMLs and increased local BMD in OA knees. Both BMLs<sup>3</sup> and increased local BMD<sup>17,18</sup> may be consequences of increased loading. As a surrogate measure of loading in the knee joint, the M:L BMD ratio was used by Lo *et al.*<sup>12</sup>. In the present study, we also investigated the relationship between the occurrence of BMLs and the M:L BMD ratio in various VOIs at different distances from the joint space. The three groups: medial BMLs, lateral BMLs and no BMLs had significantly different M:L BMD ratios for all VOIs except the juxta-physeal VOI (Table III, ANOVA). This VOI was probably too distant from the joint space to provide significant results as BMLs preferably occurred close to the joint space. The M:L BMD ratios were highest in bones with medial BMLs and lowest in bones with lateral BMLs (Table II). This illustrated the association between BMLs and increased local BMD. The M:L BMD ratio in bones with medial BMLs was lower in the cortical VOI compared to all three subchondral trabecular VOIs, which was

probably caused by BMLs mainly appearing in the cancellous bone and not in the cortical plate. In accordance, in the cortical VOI, the M:L BMD ratio in bones with medial BMLs was not significantly higher than in bones without BMLs. In a canine medial femorotibial OA model, Intema *et al.*<sup>11</sup> found that a decrease in thickness and an increase in porosity of the cortical plate were associated with cartilage lesion advancement while BMD of the subchondral trabecular bone depended on the level of loading. The significant difference between bones with lateral BMLs and bones without BMLs in the cortical VOI was probably caused by the small variance in M:L BMD ratios in the cortical VOI compared to the other VOIs. This lower variance in cortical VOIs compared to cancellous bone VOIs was in accordance with a previously reported BMD measurements precision study<sup>24</sup>. It was caused by a stricter definition of the cortical VOI compared to the other VOIs.

This study has specific advantages when compared with prior studies<sup>12–14</sup>. First, by including a control group without BMLs, we adjusted for BMD gradients in the femur and tibia, as well as the preferred occurrence of BMLs in proximity of the joint space. Second, we estimated the effect on BMD of a change in fat-water content on the specific BML tissue of interest.

The present study has several limitations. First, the uncertainty of the change of the bone marrow composition at the BML site was a major problem. According to previous studies<sup>14–16</sup>, the necrotic trabeculae which are present in BMLs potentially increase the apatite content which does not necessarily correlate with increased bone strength. Furthermore, single-energy QCT assumes a two component bone-water model and the presence of fat falsely reduces BMD values. Both the conversion of fat to water and of fat to bone reduces this error and will result in more accurate BMD values. As the fat-to-water conversion is more likely, the fat-to-

**Table II**  
Medial to lateral BMD ratios as mean  $\pm$  standard deviation for S1: subchondral epiphyseal, S2: mid-epiphyseal, S3: juxta-physeal and cortical VOIs in the femur or tibia (according to BML location), respectively (compare Fig. 4)

VOI	Medial BMLs	No BMLs	Lateral BMLs
Cortical	1.26 $\pm$ 0.21	1.17 $\pm$ 0.15	1.02 $\pm$ 0.10
S1	1.43 $\pm$ 0.38	1.17 $\pm$ 0.26	1.03 $\pm$ 0.20
S2	1.36 $\pm$ 0.54	1.09 $\pm$ 0.26	0.97 $\pm$ 0.27
S3	1.46 $\pm$ 0.83	1.13 $\pm$ 0.46	1.03 $\pm$ 0.42
Cortical + S1	1.31 $\pm$ 0.27	1.15 $\pm$ 0.21	0.99 $\pm$ 0.13
Cortical + S1 + S2	1.31 $\pm$ 0.31	1.13 $\pm$ 0.22	0.98 $\pm$ 0.17
Cortical + S1 + S2 + S3	1.32 $\pm$ 0.38	1.11 $\pm$ 0.24	0.99 $\pm$ 0.20
S1 + S2	1.40 $\pm$ 0.42	1.13 $\pm$ 0.25	1.02 $\pm$ 0.24
S1 + S2 + S3	1.41 $\pm$ 0.51	1.11 $\pm$ 0.26	1.02 $\pm$ 0.27
S2 + S3	1.40 $\pm$ 0.64	1.08 $\pm$ 0.28	1.00 $\pm$ 0.32

**Table III**  
P-values of the ANOVA and Tukey's HSD test for S1: subchondral epiphyseal, S2: mid-epiphyseal, S3: juxta-physeal and cortical VOIs in the femur or tibia (according to BML location), respectively (compare Fig. 4)

VOI	ANOVA	Tukey		
		Medial BMLs vs no BMLs	Medial BMLs vs lateral BMLs	Lateral BMLs vs no BMLs
Cortical	0.001	0.162	0.001	0.022
S1	0.001	0.009	0.002	0.369
S2	0.009	0.031	0.015	0.630
S3	0.089	0.136	0.136	0.892
Cortical + S1	0.001	0.041	0.001	0.81
Cortical + S1 + S2	0.002	0.038	0.002	0.189
Cortical + S1 + S2 + S3	0.004	0.033	0.004	0.363
S1 + S2	0.002	0.011	0.004	0.536
S1 + S2 + S3	0.005	0.015	0.012	0.731
S2 + S3	0.016	0.032	0.033	0.826



bone conversion was not simulated. Little is known concerning pathological findings associated with BMLs. There are two opposing statements. BMLs have often been associated with increased local water content<sup>19,20</sup>. However, as reported by Zanetti, edema representing water makes up only 4% of the BML region. This is supported by a study of Li *et al.*<sup>35</sup> who found that the water content between the BML and the surrounding bone marrow was not significantly different in patients with knee OA. Therefore, a pure fat-to-water conversion represents a too simplified model which gives strength to our conclusion that a true increase in BMD does exist in BML areas. Second, the CT-MR rigid registrations cannot be evaluated by an objective measure. Third, no data on varus/valgus misalignment were available.

In summary, the present study suggests an association between BMLs and increased local BMD and confirmed the findings of Lo. The M:L BMD ratio was significantly increased in medial BMLs while the decrease in lateral BMLs was not significant but this may be due to a small sample size ( $n = 13$ ).

### Authors' contributions

TL implemented the analysis framework, was involved in the study design, performed statistical analysis, interpreted the data and drafted the manuscript. OM co-implemented the analysis framework, especially the registration processes, was involved in the study design, statistical analysis, interpretation of results and manuscript revision. VB and JDL were involved in the study design, performed the BML readings, added medical expert knowledge, were involved in the interpretation of the results and manuscript revision. LL supervised the image acquisitions and managed them. WAK was involved in the design of the study. KE was involved in the design of the study, the development of the analysis method, statistical analysis, the interpretation of results and drafted the manuscript. All authors have read and approved the manuscript.

### Competing interests

The authors declare that they have no competing interests. Servier provided financial support to develop the CT software.

### References

1. Felson DT, Chaisson CE, Hill CL, Totterman SM, Gale ME, Skinner KM, *et al.* The association of bone marrow lesions with pain in knee osteoarthritis. *Ann Intern Med* 2001;134:541–9.
2. Sowers MF, Hayes C, Jamadar D, Capul D, Lachance L, Jannausch M, *et al.* Magnetic resonance-detected subchondral bone marrow and cartilage defect characteristics associated with pain and X-ray-defined knee osteoarthritis. *Osteoarthritis Cartilage* 2003;11:387–93.
3. Felson DT, McLaughlin S, Goggins J, LaValley MP, Gale ME, Totterman S, *et al.* Bone marrow edema and its relation to progression of knee osteoarthritis. *Ann Intern Med* 2003;139:330–6.
4. Baranyay FJ, Wang Y, Wluka AE, English DR, Giles GG, Sullivan RO, *et al.* Association of bone marrow lesions with knee structures and risk factors for bone marrow lesions in the knees of clinically healthy, community-based adults. *Semin Arthritis Rheum* 2007;37:112–8.
5. Zhang Y, Nevitt M, Niu J, Lewis C, Torner J, Guermazi A, *et al.* Fluctuation of knee pain and changes in bone marrow lesions, effusions, and synovitis on magnetic resonance imaging. *Arthritis Rheum* 2011;63:691–9.
6. Tanamas SK, Wluka AE, Pelletier JP, Pelletier JM, Abram F, Berry PA, *et al.* Bone marrow lesions in people with knee osteoarthritis predict progression of disease and joint replacement: a longitudinal study. *Rheumatology (Oxford)* 2010;49:2413–9.
7. Englund M, Guermazi A, Roemer FW, Yang M, Zhang Y, Nevitt MC, *et al.* Meniscal pathology on MRI increases the risk for both incident and enlarging subchondral bone marrow lesions of the knee: the MOST Study. *Ann Rheum Dis* 2010;69:1796–802.
8. Neogi T. Clinical significance of bone changes in osteoarthritis. *Ther Adv Musculoskelet Dis* 2012;4:259–67.
9. Goldring SR. Role of bone in osteoarthritis pathogenesis. *Med Clin North Am* 2009;93:25–35. xv.
10. Radin EL, Rose RM. Role of subchondral bone in the initiation and progression of cartilage damage. *Clin Orthop Relat Res* 1986;213:34–40.
11. Intema F, Hazewinkel HA, Gouwens D, Bijlsma JW, Weinans H, Lafeber FP, *et al.* In early OA, thinning of the subchondral plate is directly related to cartilage damage: results from a canine ACLT-menisectomy model. *Osteoarthritis Cartilage* 2010;18:691–8.
12. Lo GH, Hunter DJ, Zhang Y, McLennan CE, Lavalley MP, Kiel DP, *et al.* Bone marrow lesions in the knee are associated with increased local bone density. *Arthritis Rheum* 2005;52:2814–21.
13. Hunter DJ, Gerstenfeld L, Bishop G, Davis AD, Mason ZD, Einhorn TA, *et al.* Bone marrow lesions from osteoarthritis knees are characterized by sclerotic bone that is less well mineralized. *Arthritis Res Ther* 2009;11:R11.
14. Kazakia GJ, Kuo D, Schooler J, Siddiqui S, Shanbhag S, Bernstein G, *et al.* Bone and cartilage demonstrate changes localized to bone marrow edema-like lesions within osteoarthritic knees. *Osteoarthritis Cartilage* 2012;21:94–101.
15. Zanetti M, Bruder E, Romero J, Hodler J. Bone marrow edema pattern in osteoarthritic knees: correlation between MR imaging and histologic findings. *Radiology* 2000;215:835–40.
16. Modic MT, Ross JS. Lumbar degenerative disk disease. *Radiology* 2007;245:43–61.
17. Calbet JA, Moysi JS, Dorado C, Rodriguez LP. Bone mineral content and density in professional tennis players. *Calcif Tissue Int* 1998;62:491–6.
18. Bauman WA, Spungen AM, Wang J, Pierson Jr RN, Schwartz E. Continuous loss of bone during chronic immobilization: a monozygotic twin study. *Osteoporos Int* 1999;10:123–7.
19. Schett G. Bone marrow edema. *Ann N Y Acad Sci* 2009;1154:35–40.
20. Jimenez-Boj E, Nobauer-Huhmann I, Hanslik-Schnabel B, Dorotka R, Wanivenhaus AH, Kainberger F, *et al.* Bone erosions and bone marrow edema as defined by magnetic resonance imaging reflect true bone marrow inflammation in rheumatoid arthritis. *Arthritis Rheum* 2007;56:1118–24.
21. Gluer CC, Genant HK. Impact of marrow fat on accuracy of quantitative CT. *J Comput Assist Tomogr* 1989;13:1023–35.
22. Mazess RB. Errors in measuring trabecular bone by computed tomography due to marrow and bone composition. *Calcif Tissue Int* 1983;35:148–52.
23. Cooper C, Reginster JY, Chapurlat R, Christiansen C, Genant H, Bellamy N, *et al.* Efficacy and safety of oral strontium ranelate for the treatment of knee osteoarthritis: rationale and design of randomised, double-blind, placebo-controlled trial. *Curr Med Res Opin* 2012;28:231–9.
24. Zerfass P, Lowitz T, Museyko O, Bousson V, Laouisset L, Kalender WA, *et al.* An integrated segmentation and analysis approach for QCT of the knee to determine subchondral bone mineral density and texture. *IEEE Trans Biomed Eng* 2012;59:2449–58.
25. Mattes D, Haynor DR, Vesselle H, Lewellen TK, Eubank W. PET-CT image registration in the chest using free-form deformations. *IEEE Trans Med Imaging* 2003;22:120–8.

26. Insight Segmentation and Registration Toolkit, Kitware Inc., Version 3.20.
27. Kang Y, Engelke K, Kalender WA. Interactive 3D editing tools for image segmentation. *Med Image Anal* 2004;8:35–46.
28. Dice L. Measures of the amount of ecologic association between species. *Ecology* 1945;26:297–302.
29. Ranstam J. Repeated measurements, bilateral observations and pseudoreplicates, why does it matter? *Osteoarthritis Cartilage* 2012;20:473–5.
30. Ranstam J. Problems in orthopedic research: dependent observations. *Acta Orthop Scand* 2002;73:447–50.
31. Kricun ME. Red-yellow marrow conversion: its effect on the location of some solitary bone lesions. *Skeletal Radiol* 1985;14:10–9.
32. Burgener FA, Meyers SP, Tan RK, Zaunbauer W. *Differential Diagnosis in Magnetic Resonance Imaging*. Stuttgart, Germany: Georg Thieme Verlag; 2002:411.
33. Kalender WA. *Computed Tomography, Fundamentals, System Technology, Image Quality, Applications*. 3rd edn. Erlangen: Publicis; 2011.
34. Patel V, Issever AS, Burghardt A, Laib A, Ries M, Majumdar S. MicroCT evaluation of normal and osteoarthritic bone structure in human knee specimens. *J Orthop Res* 2003;21:6–13.
35. Li X, Ma BC, Bolbos RI, Stahl R, Lozano J, Zuo J, et al. Quantitative assessment of bone marrow edema-like lesion and overlying cartilage in knees with osteoarthritis and anterior cruciate ligament tear using MR imaging and spectroscopic imaging at 3 Tesla. *J Magn Reson Imaging* 2008;28:453–61.